REGULAR PAPER

Deposition Sequence Determines Morphology of C_{60} and 3,4,9,10-Perylenetetracarboxylic Diimide Islands on CaF_2(111)

Felix Loske, Michael Reichling, and Angelika Kühnle

REGULAR PAPER

Deposition Sequence Determines Morphology of C_{60} and 3,4,9,10-Perylenetetracarboxylic Diimide Islands on $CaF_2(111)$

Felix Loske, Michael Reichling[1], and Angelika Kühnle[*]

Johannes Gutenberg-Universität Mainz, Institut für Physikalische Chemie, Jakob-Welder-Weg 11, 55099 Mainz, Germany
[1]*Universität Osnabrück, Fachbereich Physik, Barbarastraße 7, 49076 Osnabrück, Germany*

The coadsorption of C_{60} and 3,4,9,10-perylenetetracarboxylic diimide (PTCDI) molecules on atomically flat terraces of the $CaF_2(111)$ surface is studied under ultra-high vacuum conditions using non-contact atomic force microscopy (NC-AFM). Deposition of PTCDI molecules on $CaF_2(111)$ yields needle-shaped, molecularly well-ordered crystals. Upon following deposition of C_{60} molecules, the PTCDI islands are completely covered by C_{60}. For the opposite deposition order, the initially grown C_{60} islands are not covered by PTCDI molecules, instead, most of the PTCDI molecules condense in pure islands, while only few PTCDI molecules nucleate at the edges of previously grown C_{60} islands. Simultaneous deposition of both molecules results in an intermixed phase with yet another island morphology. The observed fundamental differences in island morphology suggest that different dewetting barriers are involved in the formation process. © 2011 The Japan Society of Applied Physics

1. Introduction

A long-term objective of investigating molecules on surfaces is to develop strategies for creating surfaces with novel properties and functions.[1,2] In particular, molecular self-assembly has attracted great attention as a versatile tool for fabricating functional, tailor-made structures.[3] On conducting and semi-conducting surfaces, a large variety of self-assembled structures have been observed using scanning tunneling microscopy (STM) as a direct imaging technique.[3,4] When considering future applications, however, electrically insulating substrates are often mandatory, e.g., in molecular electronic devices to electronically decouple the molecular building blocks from the substrate surface. Compared to metallic substrates, the comparatively high molecular mobility on insulating surfaces largely hinders the controlled self-assembly of tailor-made molecular structures, frequently leading to clustering at step edges and the formation of bulk crystals.[5,6] So far, only very few examples exist, demonstrating a controlled molecular structure formation on the plane terrace of a bulk insulator. Recently, wire-like molecular structures have been reported to grow on $KBr(001)$[7–9] and calcite $(10\bar{1}4)$ and anchoring of a polar molecule on $CaF_2(111)$ has been demonstrated.[10,11]

The challenging task in designing molecular structures on surfaces is to choose the appropriate molecule–substrate system as the morphology and spatial distribution of molecular arrangement is not only steered by the experimental conditions such as temperature but most importantly by intrinsic properties of the molecule–substrate system parameterized by the adsorption energy and diffusion barrier. For insulating surfaces, it has been shown that the weak molecule–substrate interaction can result in dewetting of a transient non-equilibrium structure, leading to unusual island morphologies which are not obtained for a "classical" self-assembled structure on a metal surface.[12,13]

Here, we explore the potential of coadsorption of two molecular species for increasing the structural complexity in molecular self-assembly on an insulating surface, namely $CaF_2(111)$. We study molecular structures upon sequential deposition of 3,4,9,10-perylenetetracarboxylic diimide

(PTCDI) and C_{60} in dependence on the deposition order as well as upon simultaneous deposition of both molecular species. While PTCDI is known to arrange into ordered, needle-shaped islands on $NaCl(001)$,[14] C_{60} molecules form unusual islands with an aspect ratio close to unity.[12,15] Structures formed by coadsorption have, however, not yet been explored on an insulating surface.

The present study reveals distinctly different island morphologies depending on the deposition order, indicating that the dewetting barrier for C_{60} to hop on top of a preexisting PTCDI island is lower than the dewetting barrier for the reverse situation. Our work demonstrates that codeposition constitutes a promising strategy to further tune molecular structure formation on electrically insulating surfaces.

2. Experimental Procedure

Molecular structures on $CaF_2(111)$ are observed with non-contact atomic force microscopy (NC-AFM) performed at room temperature with an RHK 750 variable temperature atomic force microscope under UHV conditions following procedures outlined in ref. 15. For the images shown in this work, the oscillation amplitude was around 20 nm. The respective frequency shift setpoint (Δf_{set}) is given in the figure captions.

For each experiment, a bare $CaF_2(111)$ surface was prepared by cleavage with a procedure yielding large, atomically flat terraces so that step edges are not relevant for the present study.[16] Molecules were sublimated from home-built Knudsen cells calibrated using a quartz crystal microbalance and operated at a temperature of 540 and 530 K for PTCDI and C_{60} molecules, respectively, yielding a constant deposition rate of 0.05 ML/min. During deposition, the substrate was held at room temperature.

3. Results and Discussion

In a first step, the growth of pure PTCDI islands was analyzed, while for the structures obtained after deposition of C_{60} on $CaF_2(111)$ we refer to previous studies.[13,15] Second, we investigated the molecular structures after sequential deposition of PTCDI followed by C_{60} and *vice versa*. Finally, we investigated the structures obtained when depositing PTCDI and C_{60} molecules simultaneously.

[*]E-mail address: kuehnle@uni-mainz.de

© 2011 The Japan Society of Applied Physics
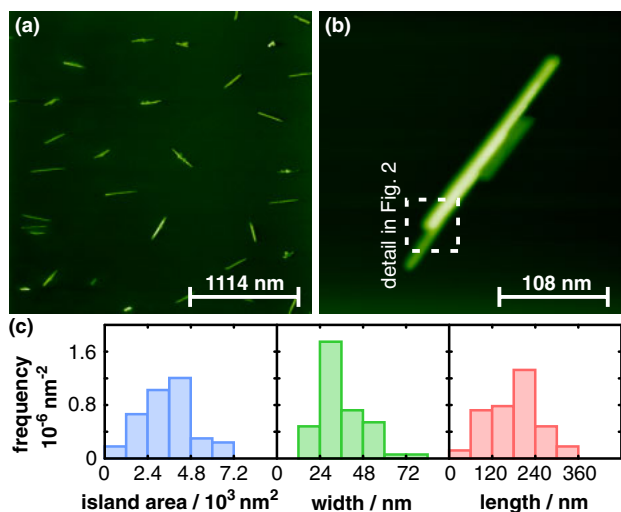
Fig. 1. (Color online) (a) NC-AFM overview image of PTCDI islands on CaF$_2$(111). The image shows a large, atomically flat terrace with islands homogeneously distributed over the surface. $\Delta f_{set} = -1.7$ Hz. (b) Individual island revealing an elongated shape and a stepped arrangement. The area enclosed by the square is shown in Fig. 2. $\Delta f_{set} = -5.0$ Hz. (c) Statistical analysis from 60 PTCDI islands.
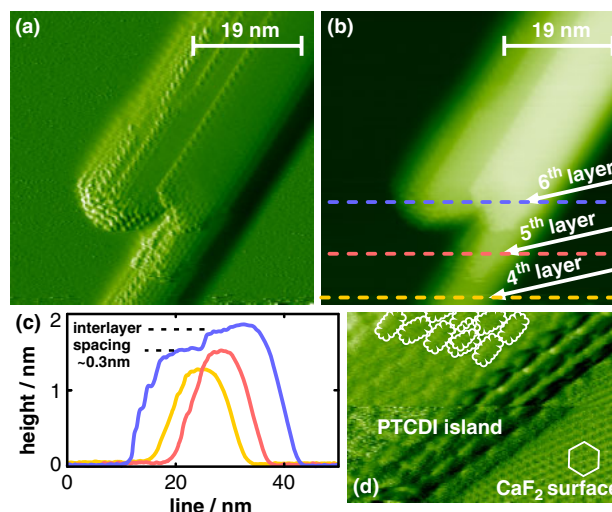

Fig. 2. (Color online) Zoom into the PTCDI island shown in Fig. 1(b). Both NC-AFM frequency shift (a) and topography (b) signals are shown. $\Delta f_{set} = -10.0$ Hz. (c) Line profiles taken from the topography image as marked by the dashed lines in (b), revealing flat, stacked PTCDI layers. (d) Within the layers, the molecules arrange in a canted phase. $\Delta f_{set} = -33.5$ Hz.

3.1 Growth of PTCDI islands

After deposition of 0.1 ML PTCDI onto freshly cleaved CaF$_2$(111) needle-like islands appear on the surface as shown in Fig. 1(a). The islands appear homogeneously distributed with an island density of approximately 4 µm^{-2}. An individual PTCDI island is shown in Fig. 1(b). A statistical analysis of sixty islands shown in Fig. 1(c) yields a mean occupied surface area of 3600–4800 nm^2. Island have mean dimensions of 30×180 nm^2, yielding a length-to-width ratio of 6. In Figs. 2(a) and 2(b), the internal structure of a PTCDI island is shown. It is apparent that the island is stepped and consists of up to six layers of PTCDI, indicating that the molecules overcome the dewetting barrier at room temperature. The interlayer spacing is about 0.3 nm, as shown in the line profiles in Fig. 2(c). Details of the molecular arrangement are shown in Fig. 2(d). The PTCDI molecules form rows, which can be explained by intermolecular hydrogen-bondings. The molecules within every second row appear rotated with respect to the molecules in the alternating rows. This so-called canted arrangement is in good agreement with the structure commonly observed for PTCDI molecules on metallic and insulating surfaces.[14,17–25] The canted arrangement is similar to the (10$\bar{2}$) surface of a bulk PTCDI crystal. This finding suggests that the PTCDI molecules are not strongly affected by the presence of the CaF$_2$(111) surface, but arrange in their own, energetically favorable bulk structure.

3.2 Sequential deposition: PTCDI followed by C$_{60}$

In a second step, we deposit C$_{60}$ molecules after deposition of PTCDI molecules. In Fig. 3(a) an overview image is shown after deposition of 0.1 ML of PTCDI followed by 0.4 ML of C$_{60}$ molecules. The observed islands appear larger than those observed for pure PTCDI deposition. Interestingly, no islands were obtained that resemble the morphol-
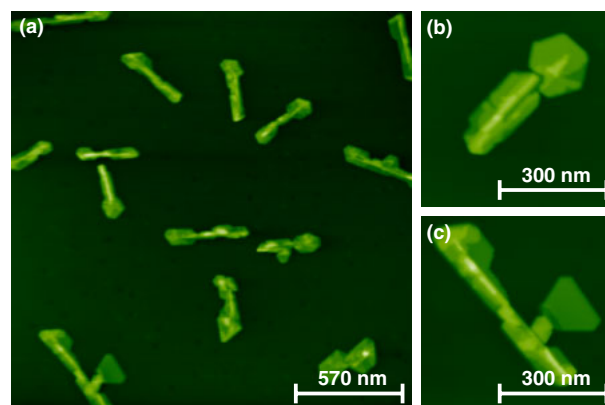
Fig. 3. (Color online) (a) Overview image of PTCDI islands covered by C$_{60}$. C$_{60}$ molecules solely nucleate at the PTCDI islands and no isolated C$_{60}$ islands are observed. $\Delta f_{set} = -0.5$ Hz. (b) and (c) represent detail images demonstrating that C$_{60}$ molecules also form larger patches attached to the elongated core. $\Delta f_{set} = -3.5$ and -1.9 Hz, respectively.

ogy obtained after deposition of only C$_{60}$ molecules.[13] Apparently, the preexisting PTCDI islands act as nucleation sites for diffusing C$_{60}$ molecules and steer the structure formation.

In Figs. 3(b) and 3(c) common island shapes are depicted. These islands consist of a narrow, elongated core, resembling the previously discussed PTCDI crystals. Around this core, larger flat islands are attached. A detailed view of the island shown in Fig. 3(c) is presented in Fig. 4(a). The stacked layers of the island are clearly visible. From line profiles given in Fig. 4(b), it is evident that the interlayer spacings are multiples of the spacing of close-packed C$_{60}$, which is 0.8 nm. In addition, the image in Fig. 4(c) shows a hexagonal arrangement with approximately 1 nm lattice constant on top of the island, corresponding to a close-
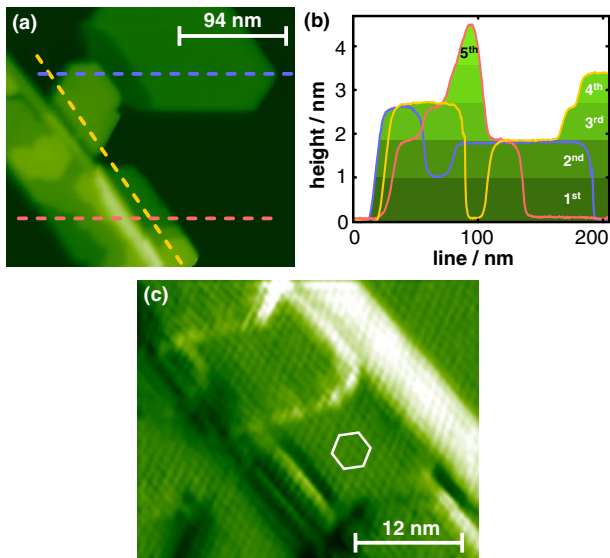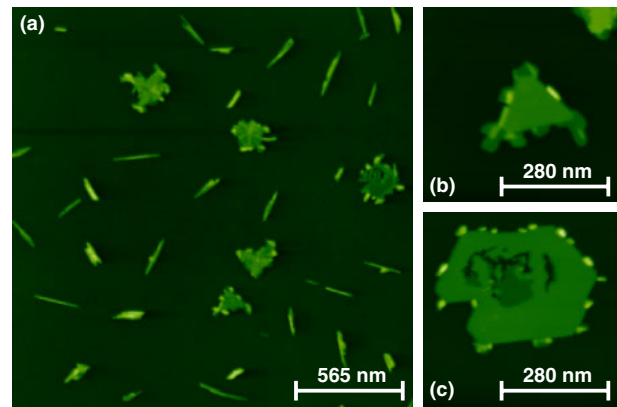
Fig. 4. (Color online) (a) Detail of Fig. 3(c), showing a C_{60} covered PTCDI island. The PTCDI core lies underneath the central elongated structure. Line profiles shown in (b) reveal an interlayer spacing of approximately 0.8 nm. Yellow and blue dashed lines profiles are taken on the C_{60} lobes next to the island while the red dashed line scan represents the PTCDI island covered by C_{60} molecules. $\Delta f_{set} = -5.1$ Hz. (c) NC-AFM image (frequency shift, low-pass filtered) on top of a C_{60} covered PTCDI island exhibiting a hexagonal molecular arrangement, identified as a close-packed C_{60} layer. $\langle \Delta f_{set} \rangle = -12.4$ Hz.

Fig. 5. (Color online) (a) Overview image of a sample initially covered with 0.1 ML of C_{60} and subsequent deposition of 0.1 ML of PTCDI. PTCDI molecules mainly arrange in needle-shaped islands and only few of them attach to the preexisting C_{60} islands. $\Delta f_{set} = -1.0$ Hz. Frames (b) and (c) show details of C_{60} islands with attached PTCDI molecules. $\Delta f_{set} = -10.0$ and -2.6 Hz, respectively.

Fig. 6. (Color online) NC-AFM image (frequency shift) of PTCDI at C_{60} island edges. PTCDI molecules arrange in a canted phase. $\langle \Delta f_{set} \rangle = -21.2$ Hz.
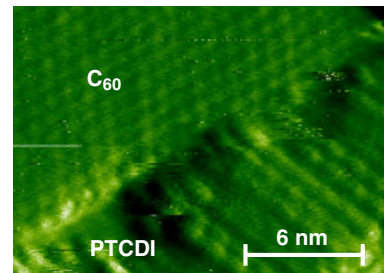
packed ordering of C_{60} molecules. This reveals that the initially grown PTCDI island is completely covered by C_{60} molecules. Moreover, patches of truncated triangular and hexagonal islands have formed around the PTCDI core. Comparing these structures to previously observed islands of pure C_{60} on $CaF_2(111)$ allows for assigning these structures to pure C_{60} islands.[13] Two important conclusions can be made from these observations. First, C_{60} molecules preferentially attach to PTCDI islands and PTCDI islands appear as nucleation seeds for the growth of pure C_{60} islands. Second, C_{60} molecules can easily hop onto preexisting PTCDI islands and they obviously overcome the respective dewetting barrier.[26]

3.3 Sequential deposition: C_{60} followed by PTCDI
Next, we change the deposition order in sequential deposition. First, 0.1 ML of C_{60} molecules were deposited, resulting in characteristic, triangular and hexagonal islands as discussed elsewhere.[13] Subsequently, 0.1 ML of PTCDI molecules were deposited. The resulting structure is shown in Fig. 5(a). Interestingly, the situation is distinctly different from the observations for the reverse deposition order. In the present case, needle-shape PTCDI islands assemble, regardless of the presence of the C_{60} islands. In particular, the majority of the PTCDI islands is not attached to C_{60} islands. Only few PTCDI clusters are observed that decorate the edges of C_{60} islands, as highlighted in the images shown in Figs. 5(b) and 5(c). Note that this observation cannot simply be explained by a restricted mobility of the PTCDI molecules, as we know from Fig. 1(a) that the molecules can overcome distances as large as several 100 nm on the surface at room temperature. In Fig. 6, an edge of a C_{60} island

decorated by PTCDI molecules is shown in detail. As can be seen, PTCDI molecules grow in a canted arrangement similar to the PTCDI bulk structure. Besides very few exceptions, no PTCDI molecules can be identified on top of C_{60} islands.

Therefore, the C_{60} islands do not act as nucleation seeds for the growth of PTCDI and, furthermore, PTCDI molecules do not hop onto the C_{60} islands, indicating that the PTCDI molecules do not wet C_{60} islands.

3.4 Simultaneous deposition
In Fig. 7(a), an image is shown after simultaneous deposition of 0.1 ML of C_{60} and PTCDI molecules. The islands appear homogeneously distributed on the surface with a density of approximately $4 \mu m^{-2}$. A zoom into a characteristic island is presented in Fig. 7(b). The observed islands have an elongated shape similar to those observed for only depositing PTCDI, however, they exhibit branches and both, the outer edges and the island surface appear rougher than PTCDI islands. This suggests a different arrangement of the PTCDI and C_{60} molecules, indicating an intermixed phase. This assignment would also explain why molecular resolution was not achieved on these islands.
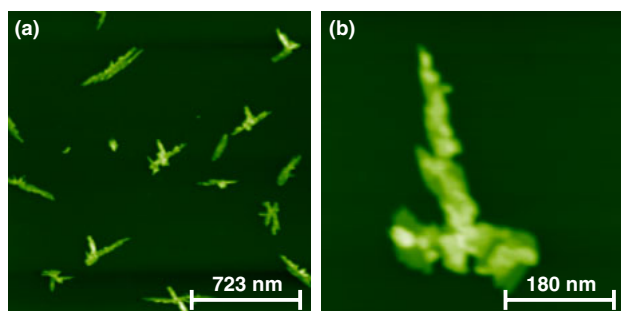
Fig. 7. (Color online) (a) Overview image of a $CaF_2(111)$ sample after simultaneous deposition of PTCDI and C_{60}. $\Delta f_{set} = -6.2\,Hz$. (b) Zoom onto a characteristic island, exhibiting a more rough surface and irregular outer shape compared to the islands observed after sequential deposition. $\Delta f_{set} = -1.3\,Hz$.

4. Conclusions

Depending on the deposition order, distinctly different island morphologies can be obtained on $CaF_2(111)$. Upon sequential deposition of C_{60} molecules onto a surface with preexisting needle-shaped PTCDI islands, the latter act as nucleation sites for diffusing C_{60} molecules. Already at a relatively low coverage of $0.4\,ML$ C_{60}, the PTCDI islands become completely covered by ordered multilayers of C_{60} molecules, indicating that the dewetting barrier is overcome at room temperature and C_{60} molecules can hop on top preexisting PTCDI islands.

In contrast, for the reverse deposition order, the preexisting triangular and hexagonal C_{60} islands do not act as nucleation sites for the growth of PTCDI islands. Rather, the majority of PTCDI molecules forms separated, needle-shaped islands, regardless of the presence of the C_{60} molecules. Hardly any PTCDI molecules are observed on top of the preexisting C_{60} islands, illustrating that PTCDI does not wet C_{60} islands.

No intermixing of PTCDI and C_{60} is observed upon sequential deposition, indicating a stable arrangement of the initially formed islands. This is in contrast to what is observed upon simultaneous deposition of both molecules. In this case, yet another structure is obtained, which is tentatively assigned to an intermixed phase. The dependence on deposition order shows that non-equilibrium structures are involved in the structure formation. Our results demonstrate that changing the deposition order can be exploited as a strategy for steering the molecular structure formation on an insulating surface.

1) C. Joachim, J. K. Gimzewski, and A. Aviram: Nature **408** (2000) 541.
2) S. R. Forrest: Nature **428** (2004) 911.
3) J. V. Barth: Annu. Rev. Phys. Chem. **58** (2007) 375.
4) A. Kühnle: Curr. Opin. Colloid Interface Sci. **14** (2009) 157.
5) T. Kunstmann, A. Schlarb, M. Fendrich, T. Wagner, R. Möller, and R. Hoffmann: Phys. Rev. B **71** (2005) 121403.
6) B. Such, T. Trevethan, T. Glatzel, S. Kawai, L. Zimmerli, E. Meyer, A. L. Shluger, C. H. M. Amijs, P. de Mendoza, and A. M. Echavarren: ACS Nano **4** (2010) 3429.
7) M. Fendrich, M. Lange, C. Weiss, T. Kunstmann, and R. Möller: J. Appl. Phys. **105** (2009) 094311.
8) S. Kawai, S. Maier, T. Glatzel, S. Koch, B. Such, L. Zimmerli, L. A. Fendt, F. Diederich, and E. Meyer: Appl. Phys. Lett. **95** (2009) 103109.
9) M. Fendrich and T. Kunstmann: Appl. Phys. Lett. **91** (2007) 023101.
10) P. Rahe, M. Nimmrich, A. Greuling, J. Schütte, I. Stará, J. Rybáček, G. Huerta-Angeles, I. Starý, M. Rohlfing, and A. Kühnle: J. Phys. Chem. C **114** (2010) 1547.
11) J. Schütte, R. Bechstein, M. Rohlfing, M. Reichling, and A. Kühnle: Phys. Rev. B **80** (2009) 205421.
12) S. A. Burke, J. M. Mativetsky, R. Hoffmann, and P. Grütter: Phys. Rev. Lett. **94** (2005) 096102.
13) M. Körner, F. Loske, M. Einax, A. Kühnle, M. Reichling, and P. Maass: Phys. Rev. Lett. **107** (2011) 016101.
14) J. M. Topple, S. A. Burke, S. Fostner, and P. Grütter: Phys. Rev. B **79** (2009) 205414.
15) F. Loske, J. Lübbe, J. Schütte, M. Reichling, and A. Kühnle: Phys. Rev. B **82** (2010) 155428.
16) L. Tröger, J. Schütte, F. Ostendorf, A. Kühnle, and M. Reichling: Rev. Sci. Instrum. **80** (2009) 063703.
17) C. Ludwig, B. Gompf, J. Petersen, R. Strohmaier, and W. Eisenmenger: Z. Phys. B **93** (1994) 365.
18) O. Guillermet, A. Glachant, J. Y. Hoarau, J. C. Mossoyan, and M. Mossoyan: Surf. Sci. **548** (2004) 129.
19) O. Guillermet, M. Mossoyan-Déneux, M. Giorgi, A. Glachant, and J. C. Mossoyan: Thin Solid Films **514** (2006) 25.
20) K. Aït-Mansour, M. Treier, P. Ruffieux, M. Bieri, R. Jaafar, P. Gröning, R. Fasel, and O. Gröning: J. Phys. Chem. C **113** (2009) 8407.
21) J. C. Swarbrick, J. Ma, J. A. Theobald, N. S. Oxtoby, J. N. O'Shea, N. R. Champness, and P. H. Beton: J. Phys. Chem. B **109** (2005) 12167.
22) B. Uder, C. Ludwig, J. Petersen, B. Gompf, and W. Eisenmenger: Z. Phys. B **97** (1995) 389.
23) F. Silly, A. Q. Shaw, M. R. Castell, and G. A. D. Briggs: Chem. Comm. (2008) 1907.
24) M. E. Cañas Ventura, W. Xiao, D. Wasserfallen, K. Müllen, H. Brune, J. V. Barth, and R. Fasel: Angew. Chem., Int. Ed. **46** (2007) 1814.
25) M. Mura, F. Silly, G. A. D. Briggs, M. R. Castell, and L. N. Kantorovich: J. Phys. Chem. C **113** (2009) 21840.
26) S. A. Burke, J. M. Topple, and P. Grütter: J. Phys.: Condens. Matter **21** (2009) 423101.

© 2011 The Japan Society of Applied Physics